

# A NEW GENERATION OF COOL WHITE DWARF ATMOSPHERE MODELS. II. A DZ STAR WITH COLLISION-INDUCED ABSORPTION

S. BLOUIN<sup>1</sup>, P. DUFOUR<sup>1</sup>, N.F. ALLARD<sup>2,3</sup>, AND M. KILIC<sup>4</sup>

*Accepted for publication in The Astrophysical Journal*

## ABSTRACT

In the first paper of this series (Blouin et al. 2018), we presented our upgraded cool white dwarf atmosphere code. In this second paper, we use our new models to analyze SDSS J080440.63+223948.6 (J0804+2239), the first DZ star to show collision-induced absorption (CIA). This object provides a crucial test for our models, since previous versions of our code were unable to simultaneously fit the metal absorption lines and the CIA. We find an excellent fit to both the spectroscopic and photometric data, which further validates the improved constitutive physics of our models. We also show that the presence of metal lines allows to lift the degeneracy between high and low hydrogen abundances that usually affects the fits of white dwarfs with CIA. Finally, we investigate the potential impact of spectroscopically undetected metals on the photometric solutions of DC stars.

*Subject headings:* stars: atmospheres — stars: individual (SDSS J080440.63+223948.6) — white dwarfs

## 1. INTRODUCTION

Most cool white dwarfs ( $T_{\text{eff}} \lesssim 5000$  K) are classified as DC stars, meaning that they have a featureless spectrum. At such temperatures, there is too little thermal energy to excite the transitions that are required to produce hydrogen or helium spectral lines in the optical and infrared. Therefore, all the information we can get from these objects is limited to photometric observations and parallaxes. This is sufficient to obtain the effective temperature  $T_{\text{eff}}$  and the surface gravity  $\log g$  by fitting the spectral energy distribution (SED) with atmosphere models (e.g., Bergeron et al. 1997, 2001). It is even possible to deduce the atmospheric composition of these objects through a detailed analysis of their SED. However, different atmosphere model codes often yield different results. For instance, Kowalski & Saumon (2006), Kilic et al. (2009a) and Kilic et al. (2009b) conclude that there are virtually no helium-rich DC stars below  $T_{\text{eff}} = 5000$  K, while the findings of Bergeron et al. (1997), Bergeron et al. (2001), Kilic et al. (2006) and Kilic et al. (2010) suggest that hydrogen and helium-rich stars are roughly equally abundant in this temperature range. These differences arise mainly because the pure helium atmosphere models of Kowalski & Saumon (2006) are similar to blackbodies, while those of the Montreal group (Bergeron et al. 2001, 1995) are not. Since cool white dwarfs do not have blackbody SEDs, using the models of Kowalski & Saumon (2006) leads to all cool DC stars being assigned a H-rich composition.

Since the featureless spectra of cool DC white dwarfs provide very few opportunities to test and compare dif-

ferent atmosphere models, problems with these models have not yet been identified. In the absence of any observational test, it is hard to say which atmosphere code should be trusted. Fortunately, cool metal-polluted white dwarfs (DZ stars) show atomic absorption lines that can be used to diagnose the accuracy of different atmosphere models. Properly fitting the spectral lines of DZ stars requires models that precisely map the temperature and density conditions of the line-forming regions of the atmosphere. This is particularly true for cool DZ stars, where spectral lines can significantly differ from conventional Lorentzian profiles (Allard et al. 2018, 2016a,b; Allard & Alekseev 2014; Allard et al. 2014). Good examples of this deviation include the Mg II 2795/2802 Å lines of van Maanen 2 (Wolff et al. 2002) and Ross 640 (Blouin et al. 2018; Koester & Wolff 2000), as well as the Na I D doublet of WD 2356-209 (Bergeron et al. 2005; Homeier et al. 2007, 2005).

Another way of diagnosing atmosphere models is to examine cool white dwarfs that show collision-induced absorption (CIA) from molecular hydrogen in the infrared (IR). CIA arises due to collisions between H<sub>2</sub> and other particles (H, H<sub>2</sub> or He), which lead to the induction of an electric dipole that enables IR absorption (Lenzuni et al. 1991; Frommhold 1994). The intensity of the IR flux depletion resulting from CIA depends mainly on the hydrogen abundance and the photospheric density, thus allowing to constrain the physical conditions in these white dwarfs. Recent theoretical calculations (Blouin et al. 2017) also show that for white dwarfs with a mixed H/He atmosphere and an effective temperature below 4000 K, the H<sub>2</sub>-He CIA profiles undergo a density-driven distortion, which could provide another way of assessing the physical conditions in the atmospheres of these objects.

In the first paper of this series (Blouin et al. 2018), we presented an improved atmosphere model code that relies on ab initio calculations to properly model cool DZ stars. We showed how this upgraded code allows better spectroscopic fits for two cool DZ stars (LP 658-2 and Ross 640) that presented a challenge to previous

<sup>1</sup> Département de Physique, Université de Montréal, Montréal 1, QC H3C 3J7, Canada; sblouin@astro.umontreal.ca, dufourpa@astro.umontreal.ca.

<sup>2</sup> GEPI, Observatoire de Paris, Université PSL, CNRS, UMR 8111, 61 avenue de l'Observatoire, 75014 Paris, France.

<sup>3</sup> Sorbonne Université, CNRS, UMR 7095, Institut d'Astrophysique de Paris, 98bis boulevard Arago, 75014 Paris, France.

<sup>4</sup> Department of Physics and Astronomy, University of Oklahoma, 440 W. Brooks St., Norman, OK 73019, USA

TABLE 1  
OBSERVATIONAL DATA.

Observation	Value
Parallax (mas)	$25.28 \pm 0.14$
<i>u</i>	$19.73 \pm 0.03$
<i>g</i>	$18.30 \pm 0.03$
<i>r</i>	$17.59 \pm 0.03$
<i>i</i>	$17.39 \pm 0.03$
<i>z</i>	$17.33 \pm 0.03$
<i>J</i>	$16.71 \pm 0.04$
<i>H</i>	$16.92 \pm 0.04$
<i>K</i>	$17.29 \pm 0.06$

atmosphere models. These improved fits suggest that our models properly capture the physics and chemistry of cool white dwarf atmospheres. To extend the validation of our code, we turn to SDSS J080440.63+223948.6 (J0804+2239), the first DZ star to show CIA. Originally identified by Kilic et al. (2010), this star has not yet been the object of any published spectroscopic or photometric fit. Since it presents both metal absorption lines and CIA, this star provides a crucial test for our models. Our detailed analysis of J0804+2239 is presented in Section 2, we discuss of the possibility of parameter degeneracies in Section 3 and our conclusions are given in Section 4.

## 2. ANALYSIS OF J0804+2239

### 2.1. Observations

Kilic et al. (2010) identified J0804+2239 as a DZ white dwarf based on a low-resolution spectrum from the Hobby-Eberly Telescope. These spectra were obtained with the Marcario Low Resolution Spectrograph (LRS; Hill et al. 1998) on UT 2005 October 30 using the G1 grism with a  $2.0''$  slit and the GG385 blocking filter. This setup provided an  $R = 300$  optical spectrum redward of  $4100 \text{ \AA}$ , which revealed significant absorption features from Ca I and the Na D doublet. The discovery of both metal lines in its optical spectrum and a significant flux deficit in the infrared prompted us to obtain a higher resolution and better quality spectrum.

We used the 6.5-m MMT with the Blue Channel Spectrograph to obtain additional spectroscopy of J0804+2239 on UT 2009 November 20. We operated the spectrograph with the  $500 \text{ line mm}^{-1}$  grating in first order, providing wavelength coverage from  $3660$  to  $6800 \text{ \AA}$  and a resolving power of  $R = 1200$  with the  $1.25''$  slit. We obtained four 3-min exposures and one 2-min exposure of the target. We obtained all spectra at the parallactic angle and acquired a He–Ar–Ne comparison lamp exposure for wavelength calibration. We used the observations of the spectrophotometric standard star G24-9, which is also a cool white dwarf, for flux calibration. Figure 1 shows the MMT spectrum of J0804+2239, which reveals additional lines from Ca II and Fe in the blue.

Our photometric analysis of J0804+2239 is based on the *ugriz* and *JHK* photometry reported in Kilic et al. (2010) and the *Gaia* DR2 parallax (Gaia Collaboration 2016, 2018), which are given in Table 1. Note that this object was also observed by the UKIDSS Large Area Survey (Lawrence et al. 2007) with photometric measurements that are consistent with those of Kilic et al. (2010) within the errors.

### 2.2. Best fit

To analyze J0804+2239, we use a new grid of atmosphere models computed using the code described in the first paper of this series (Blouin et al. 2018). This code takes into account numerous high-pressure effects relevant for the modeling of cool DZ stars. In particular, *ab initio* equations of state for helium and hydrogen are used (Becker et al. 2014), the most important spectral lines (Ca I 4226  $\text{\AA}$ , Ca II H & K, Mg I 2852  $\text{\AA}$ , Mg II 2795/2802  $\text{\AA}$ , the Mgb triplet and the Na I D doublet) are computed using the unified line shape theory of Allard et al. (1999), the nonideal ionization of helium and metals is taken into account using *ab initio* results (Kowalski et al. 2007; Blouin et al. 2018), the high-density distortion of H<sub>2</sub>–He CIA profiles is included (Blouin et al. 2017), continuum opacities are corrected for collective interactions between atoms (Rohrmann 2018; Iglesias et al. 2002) and the opacity of the far red wing of the Ly $\alpha$  line is included (Kowalski & Saumon 2006). The model grid we use to fit J0804+2239 extends in four distinct dimensions: hydrogen abundance (helium only, hydrogen only and log H/He from  $-5$  to  $0$  in steps of  $0.5$  dex), metal abundance (log Ca/He from  $-12$  to  $-8$  in steps of  $0.5$  dex), effective temperature (from  $3500$  to  $7000 \text{ K}$  in steps of  $250 \text{ K}$ ) and surface gravity (from  $7.0$  to  $9.0$  in steps of  $0.5$  dex).

We use the photometric technique (Bergeron et al. 2001) to find  $T_{\text{eff}}$ ,  $\log g$  and the hydrogen abundance of J0804+2239. In particular, the solid angle  $\pi(R/D)^2$ ,  $T_{\text{eff}}$  and the abundance ratio H/He are found using a  $\chi^2$  minimization technique based on the Levenberg-Marquardt algorithm. The photometric observations are converted into fluxes using the constants reported in Holberg & Bergeron (2006) and the evolutionary models of Fontaine et al. (2001) are used to find the mass of the star from its solid angle and parallax. Once a consistent photometric solution is found, we use the spectroscopic observations to fit the abundance of Ca, Fe and Na<sup>5</sup>. More specifically, we use the Ca II H & K and Ca I 4226  $\text{\AA}$  lines to constrain the Ca/He ratio, the small spectroscopic features near  $3700 - 3800 \text{ \AA}$  for Fe/He and the Na D doublet for Na/He. The metal abundance ratios thus found being different from our initial guesses, the photometric loop is repeated until internal consistency is reached.

The parameters of our best-fit solution are given in Table 2. The uncertainties were estimated by manually altering the solution parameters and visually inspecting the resulting fits. The corresponding spectroscopic and photometric solutions are shown in Figures 1 and 2. The spectroscopic fit is excellent: in particular, the Ca II H & K lines, the Ca I 4226  $\text{\AA}$  line and the Na D doublet are all well reproduced by our model. However, we note that our fit to the weak Fe lines is not so good. This is not surprising insofar as these lines are still computed assuming Lorentzian profiles, which are known to poorly reproduce the spectral features of cool DZ stars (Allard et al. 2018). Nevertheless, since these Fe lines are weak, they have a very limited impact on the model atmosphere structure

<sup>5</sup> All other heavy elements (from C to Cu) are included in the models, but since we could not use any spectral line to fit their abundance, we simply assumed the same abundance ratio with respect to Ca as in chondrites (Lodders 2003).

TABLE 2  
FITTING PARAMETERS.

Parameter	Value
$T_{\text{eff}}$	$4970 \pm 100$ K
$\log g$	$7.98 \pm 0.05$
$\log \text{H}/\text{He}$	$-1.6 \pm 0.2$
$\log \text{Ca}/\text{He}$	$-10.0 \pm 0.1$
$\log \text{Fe}/\text{He}$	$-9.8 \pm 0.2$
$\log \text{Na}/\text{He}$	$-11.0 \pm 0.2$
$\tau_{\text{cool}}$	$5.9 \pm 0.6$ Gyr

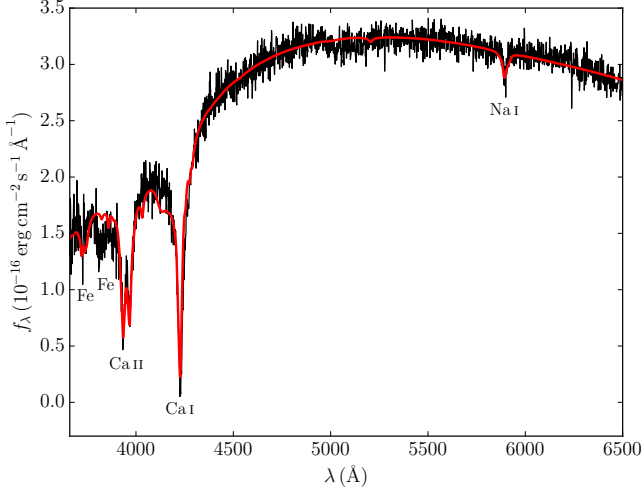


FIG. 1.— Best spectroscopic solution. The corresponding fitting parameters are given in Table 2.

and they do not affect our solution. As shown in Figure 2, the photometric fit is satisfactory: all model fluxes are within (or very close to) the observational uncertainties and the reduced  $\chi^2$  is 2.0.

Also shown in Figure 2 is the best solution found when assuming a hydrogen-free atmosphere. To obtain this solution, we used the whole fitting procedure described above to find the best  $T_{\text{eff}}$ ,  $\log g$  and metal abundances if a hydrogen-free atmosphere is assumed. This exercise clearly shows that there must be hydrogen in the atmosphere of this star, since there is no other way to generate the IR flux depletion observed in the photometric measurements.

Note that with the previous version of our atmosphere code (Dufour et al. 2007) we were unable to find a solution that simultaneously fitted both the photometry and the spectroscopy. Moreover, the atmospheric parameters of the best solution found with those models were quite different ( $T_{\text{eff}} = 4780$  K,  $\log g = 7.80$ ,  $\log \text{H}/\text{He} = -3$  and  $\log \text{Ca}/\text{He} = -10.9$ ), resulting in a cooling time of 4.2 Gyr, which is 1.7 Gyr shorter than the cooling time found with our improved models. The next section describes the improvements made to our model atmosphere code that explain the difference between both solutions.

### 2.3. On the importance of the improved constitutive physics

The density at the photosphere of our best-fitting model reaches  $0.07 \text{ g cm}^{-3}$  ( $n_{\text{He}} = 1.05 \times 10^{22} \text{ cm}^{-3}$ ). This density is low enough that many nonideal high-

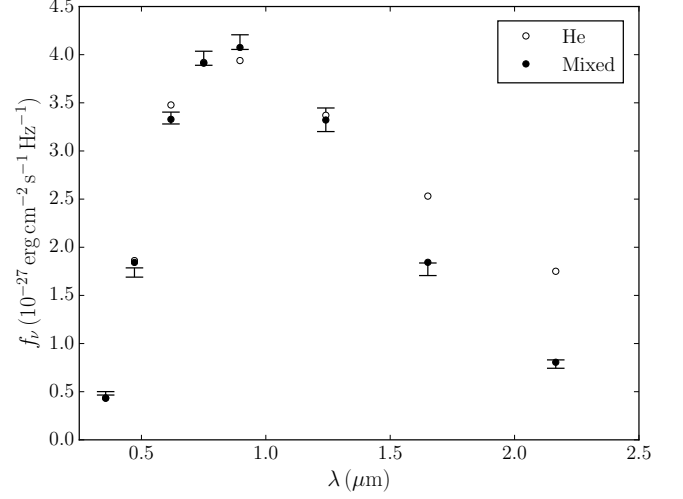


FIG. 2.— Comparison between the best photometric solution found when assuming a hydrogen-free atmosphere (open circles) and the best solution found when the H/He ratio is fitted to the photometric observations (filled circles). The atmospheric parameters of the mixed model are given in Table 2 and the hydrogen-free model has  $T_{\text{eff}} = 4620$  K,  $\log g = 7.93$  and  $\log \text{Ca}/\text{He} = -10.5$ .

density effects (e.g., nonideal ionization equilibrium, Kowalski et al. 2007; Blouin et al. 2018 and nonideal dissociation equilibrium, Kowalski 2006) are negligible. Nevertheless, the photospheric density is high enough to significantly affect spectral line profiles. Figure 3 compares the best spectroscopic solution found in the previous section to the best solution found from a model grid computed assuming Lorentzian profiles for all metal lines. Clearly, the improved profiles for Ca II H & K (Allard & Alekseev 2014) and Ca I 4226 Å lead to a much better spectral fit. Still, our Ca I 4226 Å profile is not perfect, since it predicts an unobserved small opacity bump around 4140 Å. This could be due to the fact that our Ca I 4226 Å profile was derived from interaction potentials that are not as accurate as the ones used for the rest of our improved line profiles (the Ca-He potentials were found through open-shell configuration-interaction singles calculations, using the ROCIS module of the ORCA quantum chemistry package, Neese 2011). We expect that more accurate potentials will resolve this issue.

Another improvement to the atmosphere code that proved to be crucial to obtain a good fit to J0804+2239 is the use of improved CIA profiles. As mentioned above, we use the  $\text{H}_2$ -He CIA profiles given in Blouin et al. (2017). They consist of the profiles computed by Abel et al. (2012), but corrected for various high-density non-ideal effects. Below a photospheric density of about  $0.1 \text{ g cm}^{-3}$  ( $n_{\text{He}} = 1.5 \times 10^{22} \text{ cm}^{-3}$ ), these effects are almost nonexistent and the CIA profiles used to compute our best-fitting model are therefore virtually identical to those of Abel et al. (2012). Before the implementation of these profiles, our atmosphere models were relying on the CIA profiles of Jørgensen et al. (2000). Using these profiles, we found that it is impossible to obtain a photometric solution that is as good as the one found using the profiles of Abel et al. (2012). In fact, as shown in Figure 4, the profiles of Jørgensen et al. (2000) lead to an SED that has not enough flux in the  $J$  and  $H$  bands to

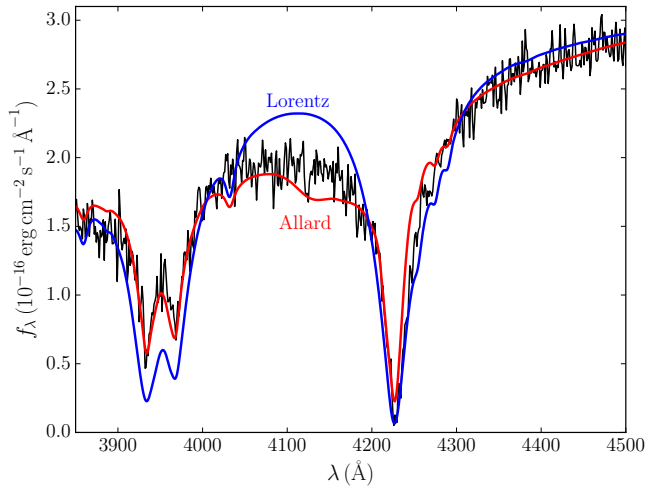


FIG. 3.— Comparison between the best solutions found when line profiles are computed using the unified line shape theory of Allard et al. (1999) (in red) and when conventional Lorentzian profiles are assumed (in blue).

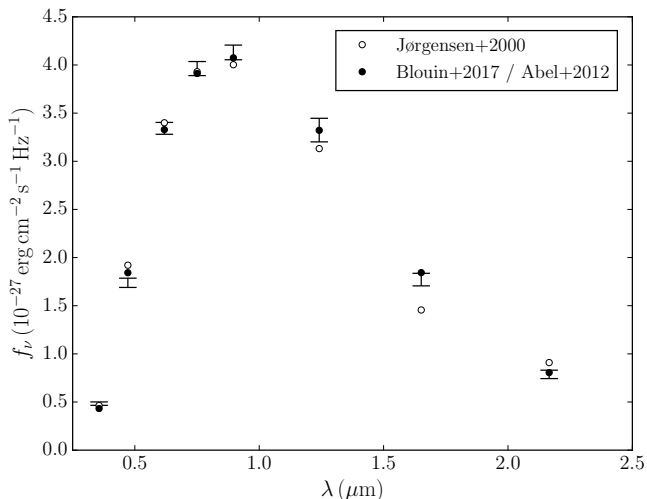


FIG. 4.— Best photometric solutions for model grids with  $\log H/He = -1.6$  and different CIA implementations. The filled circles show the solution obtained using the CIA profiles of Abel et al. (2012) or Blouin et al. (2017) (which are virtually identical for the physical conditions encountered at the photosphere of J0804+2239) and the open circles illustrate the best fit found when using the CIA profiles of Jørgensen et al. (2000).  $T_{\text{eff}}$  and  $\log g$  are adjusted to fit the photometry, while spectroscopy is used to fit the metal abundance.

fit the photometric observations. This is a direct consequence of the strong disagreement between the CIA profiles of Jørgensen et al. (2000) and Abel et al. (2012) in the  $\approx 1.2 - 2 \mu\text{m}$  region (see Figure 5). We are confident that the profiles of Abel et al. (2012) are more accurate, since Jørgensen et al. (2000) computed their CIA profiles using potential energy and induced dipole surfaces that were obtained with a smaller basis set. Moreover, using an entirely independent method (i.e., molecular dynamics with density functional theory), Blouin et al. (2017) found absorption spectra that were in better agreement with Abel et al. (2012) than with Jørgensen et al. (2000) in the  $\approx 1.2 - 2 \mu\text{m}$  interval.

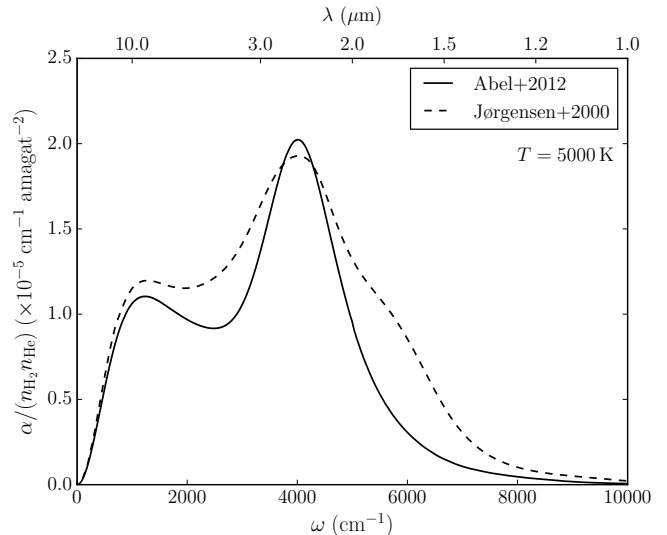


FIG. 5.—  $H_2$ -He CIA profiles at 5000 K, as computed by Abel et al. (2012) and Jørgensen et al. (2000). The spectra are divided by the number density of  $H_2$  and He.

### 3. POSSIBLE DEGENERACIES

#### 3.1. Hydrogen abundance in J0804+2239

In our atmosphere models, the intensity of the  $H_2$ -He CIA reaches a maximum when  $\log H/He \approx -2.5$ . This maximum is the result of two competing effects. On one hand, if the  $H/He$  ratio is high,  $H_2$  is more abundant and the  $H_2$ -He CIA intensity increases. On the other hand, if there is little hydrogen in the atmosphere, the density of the atmosphere is higher, which also leads to a stronger CIA. Because of this maximum,  $\chi^2$  minimization algorithms often find two solutions when fitting the photometric observations of white dwarfs with CIA in their spectrum: one above the  $\log H/He \approx -2.5$  maximum and one below. In the case of DC stars, the spectroscopic data is of no help to decide between the two solutions, so the usual approach is to simply keep the solution that has the smallest  $\chi^2$ . However, the difference between the two solutions can be quite small and minute changes in the models or in the observations can make the difference between choosing a solution instead of the other. As an example, Kilic et al. (2010) concluded that SDSS J030924.87+002525.3, SDSS J143718.15+415151.5 and SDSS J172257.78+575250.7 have, respectively,  $\log H/He$  abundance ratios of  $-4.43$ ,  $-4.26$  and  $-4.21$ , while Gianninas et al. (2015) found that the same three stars have abundance ratios of  $-1.30$ ,  $-1.97$  and  $-1.49$ .

Can our analysis of J0804+2239 also be tainted by uncertainties associated with this degeneracy of the CIA intensity? As in the examples given in the previous paragraph, we found that it is possible to obtain a second photometric solution for J0804+2239 using a hydrogen abundance below the CIA maximum at  $\log H/He \approx -2.5$ . This solution, found at  $\log H/He = -3.5$ , is shown in Figure 6. This second photometric solution is slightly better than our original solution at  $\log H/He = -1.6$ : the reduced  $\chi^2$  is 1.9. However, in order to reach the right density conditions to obtain this second solution, we had to decrease the metal abundance down to  $\log Ca/He = -11.0$ . Such a low metallicity is totally in-

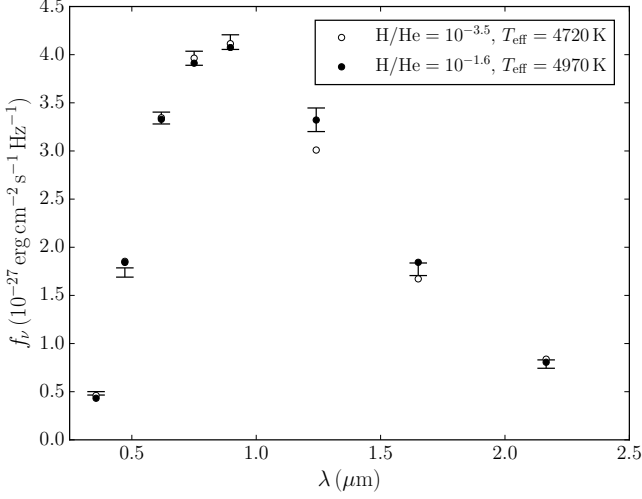


FIG. 6.— Best photometric solutions for models with  $\log \text{H/He} = -1.6$  and  $\log \text{H/He} = -3.5$ . The first solution has a metal abundance of  $\log \text{Ca/He} = -10.0$  and fits the spectroscopic data very well (Figure 1), while the second solution has a metal abundance of  $\log \text{Ca/He} = -11.0$  and is unable to reproduce the spectral lines observed in J0804+2239.

compatible with the metal lines visible in the spectrum of J0804+2239. At  $\log \text{Ca/He} = -11.0$ , the spectral lines are simply too shallow to reproduce the observed spectrum, and hence this second solution can safely be discarded. We can therefore be confident that our fit of J0804+2239 is not affected by any degeneracy related to the CIA intensity since the spectroscopic data enables us to lift this degeneracy. Note that if J0804+2239 had not shown any metal lines (as it is the case with DC stars), we could not have eliminated this degeneracy.

### 3.2. DC stars with undetected metals

In this section, we discuss of another type of degeneracy: undetectable metals in DC stars. It is well known that the inclusion of metals in atmosphere models can significantly affect the effective temperature derived from a photometric fit (compare for example the results found by Bergeron et al. 1997, 2001 to those of Dufour et al. 2005, 2007 for the same DQ and DZ samples). In this context, Figure 6 raises an interesting question. Can a spectroscopically undetectable amount of metals create a degeneracy in the photometric solution of DC stars that show CIA features? If it is the case, the atmospheric parameters of many DC stars could be wrong due to the impossibility of lifting this degeneracy.

To investigate this point, we compared *ugriz* and *JHK* photometry of atmosphere models that have the same effective temperature and hydrogen abundance, but that have different metal abundances (note that a surface gravity  $\log g = 8$  is assumed throughout this section). Figure 7 shows a sample of these comparisons for models without any heavy elements, with  $\log \text{Ca/He} = -12$  and with  $\log \text{Ca/He} = -11$ . (For a typical spectrum with a signal-to-noise ratio of 50 and a spectral resolution of  $1 \text{ \AA}$ , the spectroscopic detection threshold of metals is  $\log \text{Ca/He} \approx -11.5$ , assuming  $T_{\text{eff}}$  and  $\text{H/He}$  values similar to the models of Figure 7.) We notice that the SEDs of models with a relatively high hydrogen abundance ( $\log \text{H/He} = -2$ ) are barely affected by the

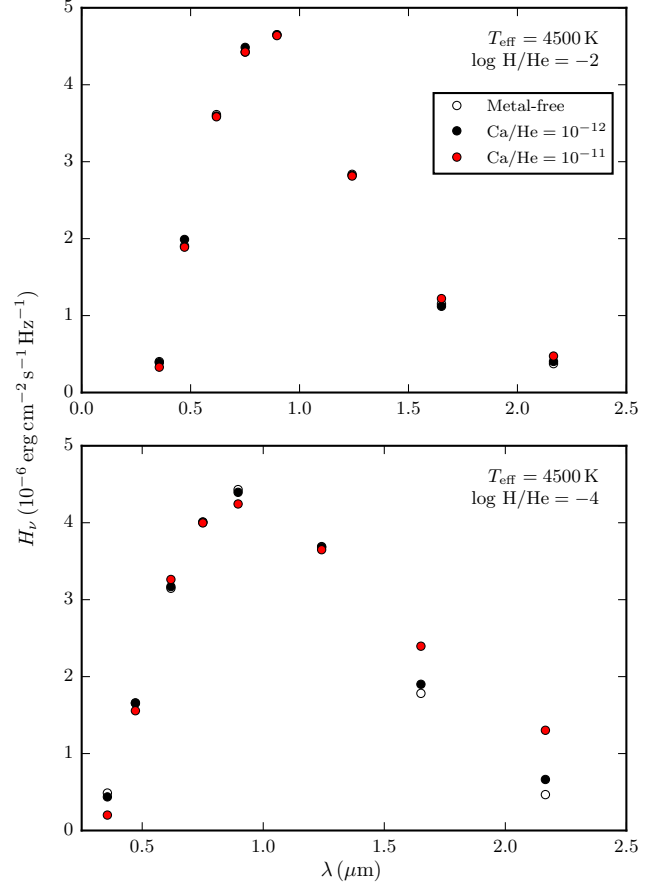


FIG. 7.— *ugriz* and *JHK* photometry of atmosphere models with  $T_{\text{eff}} = 4500 \text{ K}$  and  $\log g = 8$ . The top panel shows SEDs of models with  $\log \text{H/He} = -2$  and the bottom one those of  $\log \text{H/He} = -4$  models. On each panel, we compare the SEDs of models with different metal abundances, as indicated in the legend. For the top panel, note that the metal-free SED is virtually identical to the SED with  $\log \text{Ca/He} = -12$ .

addition of heavy elements, while the SEDs of models with a lower hydrogen abundance ( $\log \text{H/He} = -4$ ) are much more affected. There are two reasons for this difference. First, hydrogen is much less transparent than helium. As a result, for a model with little hydrogen, it does not take a lot of heavy elements before we start "seeing" metals in the SED. Secondly, the atmosphere model structure is less affected by the addition of metals for the  $\log \text{H/He} = -2$  models since hydrogen provides most of the free electrons, which largely control continuum opacities and the photospheric pressure. For the  $T_{\text{eff}} = 4500 \text{ K}$ ,  $\log \text{H/He} = -2$  and  $\log \text{Ca/He} = -11$  model, hydrogen atoms provide 96.9% of the free electrons at the photosphere, while heavy elements account for a mere 3.1%. Since the addition of metals barely affects the free electron density, it is unsurprising that it hardly affects the SED. On the opposite, for the  $T_{\text{eff}} = 4500 \text{ K}$ ,  $\log \text{H/He} = -4$  and  $\log \text{Ca/He} = -11$  model, heavy elements provide 23.4% of the free electrons at the photosphere and can therefore significantly influence the atmosphere model structure.

From our analysis of Figure 7, we can conclude that for stars with a relatively high hydrogen abundance there is no danger of solution degeneracies caused by a spec-

troscopically undetectable amount of metals. However, for DC stars with a smaller amount of hydrogen (e.g.,  $\log H/He = -4$ ), the SED is changed even when a spectroscopically undetectable amount of metals is added to the atmosphere and there is therefore a risk of finding an erroneous photometric solution. In other words, it is a priori possible that fitting a white dwarf that has a small quantity of metals (e.g.,  $\log Ca/He = -12$ ) using metal-free models yields an effective temperature and hydrogen abundance that are incorrect given that the influence of metals on the atmosphere structure of this hypothetical star was not taken into account.

If this scenario has a chance to come true, then it should be possible for a metal-free model to emulate the SED of a model with a small quantity of metals and a different  $T_{\text{eff}}$  and H/He abundance ratio. To test if it is the case, we tried to fit the SEDs of cool DZ stars using a grid of helium-rich DC models. For these fits, both the effective temperature and the H/He ratio were adjusted. We explored a parameter space extending from  $T_{\text{eff}} = 4000$  to  $5500$  K, from  $\log H/He = -6$  to  $-3$ , and from  $\log Ca/He = -13$  (well below the detection threshold) to  $-11$  (slightly above the detection threshold). In the worst case, we find that the effective temperature obtained by the fitting procedure has a  $250$  K discrepancy with the actual temperature of the DZ model that is being fitted. More important are the discrepancies found on H/He (which can reach 3 dex), but this is simply a manifestation of the CIA degeneracy described in Section 3.1 and not an effect attributable to the presence of metals in the atmosphere. Therefore, we can conclude that the degeneracy due to the presence of undetected metals does not generate errors that go beyond the usual fitting uncertainties.

Note that these conclusions also extend to DC stars that do not show any CIA feature ( $\log H/He < -5$ ). This result is quite different than what was previously found using the models of Dufour et al. (2007). Figure 8 shows how the SED of those models are affected by the addition of a small amount of metals. At  $T_{\text{eff}} = 4000$  K, a metal abundance as low as  $\log Ca/He = -12$  leads to drastic differences in the shape of the SED. As shown in Figure 8, such a difference is not visible with our improved models. The main explanation for the disagreement between both sets of models lies in the atmosphere model structure of pure-helium models. In particular, as the pressure ionization of helium (Kowalski et al. 2007) was not implemented in the models of Dufour et al. (2007), their pure-helium models are much more transparent than our new models. The photospheric pressure reaches  $10^{13}$  dyn/cm<sup>2</sup> for  $T_{\text{eff}} = 4000$  K, more than 20 times the pressure of a model with  $\log Ca/He = -12$ . On the contrary, with our improved models, the model atmosphere structure without metals and with  $\log Ca/He = -12$  are very similar. Because of the pressure ionization of helium, free electrons are still abundant when metals are absent. For that reason, the intensity of He<sup>+</sup> free-free absorption does not fall dramatically as it is the case with the models of Dufour et al. (2007).

#### 4. CONCLUSION

We presented the first spectroscopic and photometric fit of J0804+2239, a unique cool DZ star that shows CIA.

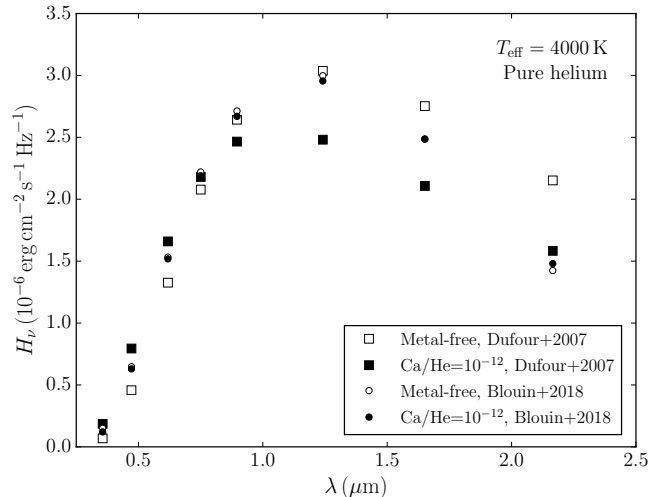


FIG. 8.— SEDs of hydrogen-free atmosphere models with  $T_{\text{eff}} = 4000$  K and  $\log g = 8$ . The circles correspond to the results obtained using the models of Blouin et al. (2018) and the squares to those found with the models of Dufour et al. (2007). For the later, note how the SED changes when a minute amount of metals is added to the atmosphere.

The improvements recently made to our atmosphere code (in particular, the improved high-pressure Ca line profiles and the new H<sub>2</sub>-He CIA profiles) proved to be crucial to obtain a good fit. These results show that our upgraded code properly captures the physics of the moderately dense atmospheres of cool DZ stars.

Because it contains metals, the hydrogen abundance in the atmosphere of J0804+2239 could be determined with greater certainty than the hydrogen abundance of most white dwarfs with CIA features. In fact, the presence of metal absorption lines lifts the degeneracy between high and low hydrogen abundances. We also explored the possibility that spectroscopically undetected metals could affect the photometric solutions of DC stars. We found that in the worst case the errors induced on the atmospheric parameters are of the order of the usual fit uncertainties.

In the next paper of this series, we will continue the observational validation of our model atmosphere code with still cooler DZ stars. In particular, we will revisit WD 2356-209, a cool DZ with an atypically strong Na D doublet.

This work was supported in part by NSERC (Canada). This work has made use of the Montreal White Dwarf Database (Dufour et al. 2017).

This work has made use of data from the European Space Agency (ESA) mission *Gaia* (<https://www.cosmos.esa.int/gaia>), processed by the *Gaia* Data Processing and Analysis Consortium (DPAC, <https://www.cosmos.esa.int/web/gaia/dpac/consortium>). Funding for the DPAC has been provided by national institutions, in particular the institutions participating in the *Gaia* Multilateral Agreement.

## REFERENCES

- Abel, M., Frommhold, L., Li, X., & Hunt, K. L. C. 2012, *J. Chem. Phys.*, 136, 044319
- Allard, N. F., & Alekseev, V. A. 2014, *Advances in Space Research*, 54, 1248
- Allard, N. F., Guillon, G., Alekseev, V. A., & Kielkopf, J. F. 2016a, *A&A*, 593, A13
- Allard, N. F., Homeier, D., Guillon, G., Viel, A., & Kielkopf, J. 2014, *Journal of Physics: Conference Series*, 548, 012006
- Allard, N. F., Kielkopf, J. F., Blouin, S., et al. 2018, *ArXiv e-prints*, arXiv:1809.04531
- Allard, N. F., Leininger, T., Gad  a, F. X., Brousseau-Couture, V., & Dufour, P. 2016b, *A&A*, 588, A142
- Allard, N. F., Royer, A., Kielkopf, J. F., & Feautrier, N. 1999, *Phys. Rev. A*, 60, 1021
- Becker, A., Lorenzen, W., Fortney, J. J., et al. 2014, *ApJS*, 215, 21
- Bergeron, P., Leggett, S. K., & Ruiz, M. T. 2001, *ApJS*, 133, 413
- Bergeron, P., Ruiz, M. T., Hamuy, M., et al. 2005, *ApJ*, 625, 838
- Bergeron, P., Ruiz, M. T., & Leggett, S. K. 1997, *ApJS*, 108, 339
- Bergeron, P., Saumon, D., & Wesemael, F. 1995, *ApJ*, 443, 764
- Blouin, S., Dufour, P., & Allard, N. F. 2018, *ApJ*, 863, 184
- Blouin, S., Kowalski, P. M., & Dufour, P. 2017, *ApJ*, 848, 36
- Dufour, P., Bergeron, P., & Fontaine, G. 2005, *ApJ*, 627, 404
- Dufour, P., Blouin, S., Coutu, S., et al. 2017, in *Astronomical Society of the Pacific Conference Series*, Vol. 509, 20th European White Dwarf Workshop, ed. P.-E. Tremblay, B. Gaensicke, & T. Marsh, 3
- Dufour, P., Bergeron, P., Liebert, J., et al. 2007, *ApJ*, 663, 1291
- Fontaine, G., Brassard, P., & Bergeron, P. 2001, *PASP*, 113, 409
- Frommhold, L. 1994, *Collision-Induced Absorption in Gases* (Cambridge University Press), doi:10.1017/cbo9780511524523
- Gaia Collaboration. 2016, *A&A*, 595, A1
- . 2018, *A&A*, 616, A1
- Gianninas, A., Curd, B., Thorstensen, J. R., et al. 2015, *MNRAS*, 449, 3966
- Hill, G. J., Nicklas, H. E., MacQueen, P. J., et al. 1998, in *Proc. SPIE*, Vol. 3355, *Optical Astronomical Instrumentation*, ed. S. D’Odorico, 375–386
- Holberg, J. B., & Bergeron, P. 2006, *AJ*, 132, 1221
- Homeier, D., Allard, N., Allard, F., et al. 2005, in *Astronomical Society of the Pacific Conference Series*, Vol. 334, 14th European Workshop on White Dwarfs, ed. D. Koester & S. Moehler, 209
- Homeier, D., Allard, N., Johnas, C. M. S., Hauschildt, P. H., & Allard, F. 2007, in *Astronomical Society of the Pacific Conference Series*, Vol. 372, 15th European Workshop on White Dwarfs, ed. R. Napiwotzki & M. R. Burleigh, 277
- Iglesias, C. A., Rogers, F. J., & Saumon, D. 2002, *ApJ*, 569, L111
- J  rgensen, U. G., Hammer, D., Borysow, A., & Falkesgaard, J. 2000, *A&A*, 361, 283
- Kilic, M., Kowalski, P. M., Reach, W. T., & von Hippel, T. 2009a, *ApJ*, 696, 2094
- Kilic, M., Kowalski, P. M., & von Hippel, T. 2009b, *AJ*, 138, 102
- Kilic, M., Munn, J. A., Harris, H. C., et al. 2006, *AJ*, 131, 582
- Kilic, M., Leggett, S. K., Tremblay, P.-E., et al. 2010, *ApJS*, 190, 77
- Koester, D., & Wolff, B. 2000, *A&A*, 357, 587
- Kowalski, P. M. 2006, *ApJ*, 641, 488
- Kowalski, P. M., Mazevet, S., Saumon, D., & Challacombe, M. 2007, *Phys. Rev. B*, 76, 075112
- Kowalski, P. M., & Saumon, D. 2006, *ApJ*, 651, L137
- Lawrence, A., Warren, S. J., Almaini, O., et al. 2007, *MNRAS*, 379, 1599
- Lenzuni, P., Chernoff, D. F., & Salpeter, E. E. 1991, *ApJS*, 76, 759
- Lodders, K. 2003, *ApJ*, 591, 1220
- Neese, F. 2011, *Wiley Interdisciplinary Reviews: Computational Molecular Science*, 2, 73
- Rohrman, R. D. 2018, *MNRAS*, 473, 457
- Wolff, B., Koester, D., & Liebert, J. 2002, *A&A*, 385, 995